

MEMORANDUM
RM-5301-ARPA
AUGUST 1967

A MODEL FOR THE GENERATION OF
MAGNETOHYDRODYNAMIC WAVES BY
HIGH-ALTITUDE NUCLEAR BURSTS

R. F. Lutomirski

PREPARED FOR:
ADVANCED RESEARCH PROJECTS AGENCY

The RAND *Corporation*
SANTA MONICA • CALIFORNIA

MEMORANDUM
RM-5301-ARPA
AUGUST 1967

A MODEL FOR THE GENERATION OF
MAGNETOHYDRODYNAMIC WAVES BY
HIGH-ALTITUDE NUCLEAR BURSTS

R. F. Lutomirski

This research is supported by the Advanced Research Projects Agency under Contract No. DAHC15 67 C 0141. Any views or conclusions contained in this Memorandum should not be interpreted as representing the official opinion or policy of ARPA.

DISTRIBUTION STATEMENT

Distribution of this document is unlimited.

PREFACE

This analysis was conducted for the Advanced Research Projects Agency as part of RAND's continuing study of the detection of nuclear explosions. It examines in detail the characteristics of the hydro-magnetic signal produced by a high-altitude nuclear explosion and the generation mechanism for an assumed model of the expanding debris.

This Memorandum should be of interest to those concerned with geophysical effects due to nuclear detonations and with the detection of these explosions.

SUMMARY

This Memorandum advances a theory for the generation of magneto-hydrodynamic (MHD) waves by a high-altitude nuclear explosion. These waves have been judged responsible for oscillations of the geomagnetic field in the frequency range of about .01 to 10 Hz. For a simple model of the debris expanding at a velocity less than the local Alfven speed into the ionosphere-exosphere, the dependence of the MHD signal strength on the yield-to-mass ratio of the device is obtained. The system is demonstrated to radiate, and the MHD radiation, with its power spectral density, is calculated. It is pointed out that the MHD radiation can, in certain cases, be very much less than the hydromagnetic yield. In addition, that portion of the hydromagnetic yield which does not appear as radiation is interpreted physically, and conservation of energy is demonstrated.

The theory predicts that the greater the yield-to-mass ratio of the device, the stronger the MHD signal produced, and, consequently, the easier it will be to detect. Further, the signal radiated from a given device (with specified hydromagnetic yield and mass) is shown to decrease as the local Alfven speed at the burst height increases, and an altitude profile of the radiation from a specified device is presented together with some examples illustrating applications of the theory.

CONTENTS

PREFACE	iii
SUMMARY	v
LIST OF FIGURES	ix
Section	
I. INTRODUCTION	1
II. PHYSICAL MODEL	4
III. MATHEMATICAL FORMULATION AND DISCUSSION	6
IV. THE ZERO-ORDER FIELDS	12
V. ENERGY CONSIDERATIONS AND RADIATION	19
Example 1	28
Example 2	31
Example 3	31
VI. THE FIRST-ORDER AND TOTAL FIELDS	33
VII. CONCLUSIONS	36
Appendix	
A. CALCULATION OF THE ZERO-ORDER FIELDS	37
B. DIRECT CALCULATION OF THE WORK DONE IN EXPANDING THE SPHERE FROM THE STRESS TENSOR	41
C. CALCULATION OF THE FIRST-ORDER FIELDS	44
REFERENCES	47

LIST OF FIGURES

1. Cylindrical and spherical coordinate systems with origin at the center of the conductor and z axis parallel to \underline{B}_0	9
2. The radial component of induced magnetic field versus retarded time $\eta = t - r/S$	14
3. The θ component of induced magnetic field versus η	15
4. The induced electric field E_φ versus η	16
5. Surface current density j_s versus time t	17
6. Expansion radius a versus β for a fixed hydromagnetic yield Y_H	24
7. Expansion time τ versus β for a fixed hydromagnetic yield Y_H	25
8. Radiation efficiency W_R/Y_H versus β for a fixed hydromagnetic yield Y_H	27
9. Frequency spectrum of hydromagnetic radiation $W_R(\omega)$ per solid angle versus $\omega\tau$	29
10. Radiation efficiency W_R/Y_H versus altitude using a nighttime sunspot minimum altitude profile for the Alfven speed	30

I. INTRODUCTION

The existence of low-frequency fluctuations in the geomagnetic field generated by both high-altitude nuclear explosions and naturally occurring phenomena has been of interest for some time. These ground-level oscillations obviously depend upon the characteristics of both the source of the disturbance and the transmission medium. Assuming a steady-state source, a number of authors⁽¹⁻⁵⁾ have calculated transmission coefficients in the frequency range of about .01 to 10 Hz. In addition, a time-dependent ground-level signal from an impulse source has been computed using a one-dimensional model for the system consisting of the earth, ionosphere, and exosphere.^(6,7) These treatments show that the time behavior of the measured signal depends largely on the resonant frequencies of the transmission coefficients of the system. However, little can be said concerning the amplitude of the ground signal from a high-altitude burst until more is known about the strength of the generated hydromagnetic signal as a function of the source height, yield, and mass. Thus, to supplement the previous work, which has been primarily concerned with propagation mechanisms, the intent of this Memorandum is to examine separately certain features of the signal which are attributable to the characteristics of the source. In particular, the question of what fraction of the total hydromagnetic yield is radiated from a bomb as hydromagnetic energy will be considered. However, no attempt will be made here to study the propagation problem in any detail.

For the purpose of this analysis, a simple mathematical model has been chosen which should adequately represent the gross features of the expanding debris after a high-altitude detonation. A brief physical description of the problem is given in Section II. In Section III, the appropriate wave equations are derived. For the idealized propagation medium considered, it is pointed out that to lowest order in the ratio of wave frequency to ion-cyclotron frequency, ω/Ω_i , only the fast, or isotropic, mode is excited. Using this same ratio as an expansion parameter in a perturbation expansion, the fast mode can then be used as a source term for exciting the slow or anisotropic mode. While Argus measurements^(8,9) indicate that the dominant ground level signal contained a considerable anisotropic component, a more realistic inhomogeneous propagation medium (i.e., the ionosphere-exosphere) could couple these anisotropic modes more strongly to the waves considered here. A detailed comparison between theory and data cannot be made until the present treatment is coupled with a realistic analysis of the propagation problem.

In Section IV, the zero-order electromagnetic fields (which are derived in Appendix A) are presented with their respective Fourier transforms and the surface current density.

Section V presents a calculation of the magnetohydrodynamic (MHD) energy radiated from the source, and of the corresponding power spectrum. Conservation of energy is discussed, and the total work done in expanding the device is calculated directly from the stress tensor in Appendix B. The MHD radiation efficiency of the device is then defined as the ratio of true MHD radiation to hydromagnetic yield,

and examples are given for some assumed yield-to-mass ratios and for a model ionosphere-exosphere. For very-high-altitude bursts, the ground level signal will be predominately affected by the radiation fields. It is pointed out that, for a given hydromagnetic yield Y_H and debris expansion velocity V , the radiation increases monotonically with the ratio V/S , where S is the local Alfvén speed. For bursts in regions where the Alfvén speed is very large, the radiated hydromagnetic energy can be much less than Y_H . Possible large variations of hydromagnetic radiation with height are also demonstrated. For example, it is pointed out that if a daytime burst with an Argus type yield and mass had been exploded at 2000 km instead of at about 480 km, the hydromagnetic radiation would have been diminished by almost two orders of magnitude. This, of course, has strong implications with regard to detection.

In Section VI, the first-order problem is formulated, and a discussion of the first-order and total electromagnetic fields is presented (these are derived in Appendix C).

II. PHYSICAL MODEL

In a nuclear explosion, the liberation of large amounts of energy in a small period of time results in the bomb materials' being heated to several million degrees, forming a dense plasma. The highly conducting gas initially will expand freely into the surrounding medium at a rate of typically hundreds of kilometers per second, pushing the earth's magnetic field lines aside. In this Memorandum, primary interest will be in this initial behavior of the plasma, which for typical bursts^(7,10) occurs for periods on the order of a fraction of a second. Later, as the volume increases, the surface stresses due to the distorted magnetic field increase, while the internal kinetic pressure decreases due to the decrease in ion concentration. The restoring force thus increases with the radius, and oscillations could occur. Instabilities and recombination processes may also affect the later expansion stages. In addition, the surface stresses due to the confining magnetic field are not spherically symmetric, and the plasma will eventually become elongated in the direction of the field.

A large fraction of the total yield will be radiated essentially instantaneously as X-rays, resulting in ionization being produced in the D and lower E layers of the ionosphere, which can greatly effect propagation in these regions. In this Memorandum, primary interest is in the generation rather than the ionospheric propagation of MHD waves from bursts above the E layer, and X-ray effects will not be of concern in this regard.

A number of authors^(7,10,11) have considered the geomagnetic effects produced by a static diamagnetic sphere as a model for the plasma cloud. The radius of expansion has been approximately estimated by equating the hydromagnetic yield, Y_H , of the bomb to the magnetic energy expelled by the conductor. From a knowledge of the mass of the bomb products, a mean expansion velocity and, hence, expansion time may be estimated. As far as is known, no estimates have been made of the fraction of Y_H which is emitted as MHD radiation.

In this paper, the plasma is taken to be a perfectly conducting sphere which expands with uniform velocity V for a time τ and then immediately comes to rest. The plasma medium interface is assumed to be sharp, and is the site of eddy currents which keep the geomagnetic field from penetrating the plasma.

The sphere is considered to expand at a velocity much less than the Alfven speed, S , into a homogeneous plasma immersed in a uniform magnetic field. While the first assumption limits the yield-to-mass ratios for which the analysis can be applied, there are some realistic cases for which this criterion is well satisfied. The plasma medium is considered to be infinite, cold, and collisionless, with the relevant electromagnetic properties represented by a dielectric tensor. This representation, and the mathematical formulation of the pertinent equations, are discussed in Section III.

III. MATHEMATICAL FORMULATION AND DISCUSSION

In the linear hydromagnetic approximation, outside of a sphere of a radius St , where t is time measured after burst, the medium is quiescent, and the magnetic field, $B_0 \underline{e}_z$, is constant in space and time. Over most of the medium, the magnetic field will be perturbed very little from its equilibrium value, and a linearized theory is appropriate. Within the framework of linear theory, the equations of motion for each plasma component can easily be solved to compute the dielectric tensor of the medium.

In order to solve the problem self-consistently, it is necessary to express the currents, or particle velocities, in terms of the fields everywhere, near the surface of the sphere as well as far from it. Near the sphere, however, the time-dependent magnetic field induced by the moving conductor cannot be neglected in comparison to B_0 . In fact, the induced field must be of the order B_0 at the surface in order that the total radial component of \underline{B} vanish there (see Eq. (6a)). Such an approach therefore leads to nonlinear equations for the particle velocities near the sphere.

However, by using linear theory near the sphere as well as far from it, it is found that the fields thus calculated have the correct order of magnitude at the surface (i.e., $|\underline{B}| \sim B_0$, $|\underline{E}| \sim VB_0$), and that the boundary conditions can be exactly satisfied. The surface current density, the particle trajectories, and hence the currents in the medium, must then be approximately correct near the sphere. However, the greater the distance from the surface of the sphere, the

more correct a linearized description of the properties of the medium becomes. For distances greater than approximately two radii, the functional dependence of the fields on distance must be quite accurate since linear theory then becomes an excellent approximation. Therefore, a calculation based solely upon linearized theory would yield correct results everywhere, at least within an order of magnitude.

The equations governing the propagation of waves at frequencies $0 \leq \omega \lesssim \Omega_i$ (where $\Omega_i = ZeB_0/M_i$, the ion-cyclotron frequency in MKS units, Ze is the ionic charge, and M_i is the ionic mass) are now derived. The dielectric tensor can be written for a Cartesian coordinate system as⁽¹²⁾

$$\underline{\underline{K}} = \begin{pmatrix} K_1 & K_2 & 0 \\ -K_2 & K_1 & 0 \\ 0 & 0 & K_3 \end{pmatrix} \quad (1)$$

where

$$K_1 = 1 + \frac{\omega_{pi}^2}{\Omega_i^2 - \omega^2}, \quad K_2 = \frac{i\omega}{\Omega_i} \frac{\omega_{pi}^2}{\Omega_i^2 - \omega^2}, \quad K_3 = -\frac{\omega_{pe}^2}{\omega^2} \quad (2)$$

Here ω_{pi} and ω_{pe} are the ion and electron plasma frequencies, respectively, a time dependence of $e^{-i\omega t}$ has been assumed, and terms of the order of electron to ion mass have been neglected. The wave equation for the electric field may be written as

$$\nabla \times \nabla \times \underline{\underline{\tilde{E}}} = \frac{\omega^2}{c^2} \underline{\underline{K}} \cdot \underline{\underline{\tilde{E}}} \quad (3)$$

Transforming to cylindrical coordinates with z axis through the center of the sphere (see Fig. 1), the dielectric tensor $\underline{\underline{K}}$ is unaltered, with the rows and columns now labelled (ρ, φ, z) . In addition, for $\omega/\Omega_i \ll 1$ and $\Omega_i \ll \omega_{pi} \ll \omega_{pe}$, $K_3 \gg K_1, K_2$. On a relative scale, as $K_3 \rightarrow \infty$, the plasma becomes infinitely conducting in the direction of the zero-order magnetic field, and from Eqs. (1) and (3), $E_z \rightarrow 0$. In this limit, the φ and ρ components of Eq. (3) yield, respectively,

$$-(\nabla \times \nabla \times \underline{\underline{E}})_{\varphi} + \frac{K_1 \omega^2}{c^2} \tilde{E}_{\varphi} = \frac{K_2 \omega^2}{c^2} \tilde{E}_{\rho} \quad (4a)$$

$$\frac{\partial^2 \tilde{E}_{\rho}}{\partial z^2} + \frac{K_1 \omega^2}{c^2} \tilde{E}_{\rho} = - \frac{K_2 \omega^2}{c^2} \tilde{E}_{\varphi} \quad (4b)$$

In the limit $\omega/\Omega_i \rightarrow 0$, $K_1 \rightarrow 1 + \rho_m/\epsilon_0 B_0^2 \equiv c^2/S^2$, and $K_2 \rightarrow 0$, where S is the Alfvén velocity and ρ_m is the mass density of the plasma. In this very low frequency or hydromagnetic regime, the medium is nondispersive, and Eqs. (4a) and (4b) become decoupled for the two familiar MHD modes of propagation. The excitation of the slow mode, \tilde{E}_{ρ} , which propagates along the field lines, is dependent upon the source containing a current in the z direction. ⁽¹³⁾

For the problem under consideration, the fields are essentially those of a radiating magnetic dipole with moment aligned antiparallel to \underline{B}_0 with surface currents (as well as the plasma currents) in the φ direction. In this regime, the slow mode is therefore not excited at all. Treating ω/Ω_i as a small parameter in a perturbation expansion, the isotropic (fast) mode is coupled to the anisotropic

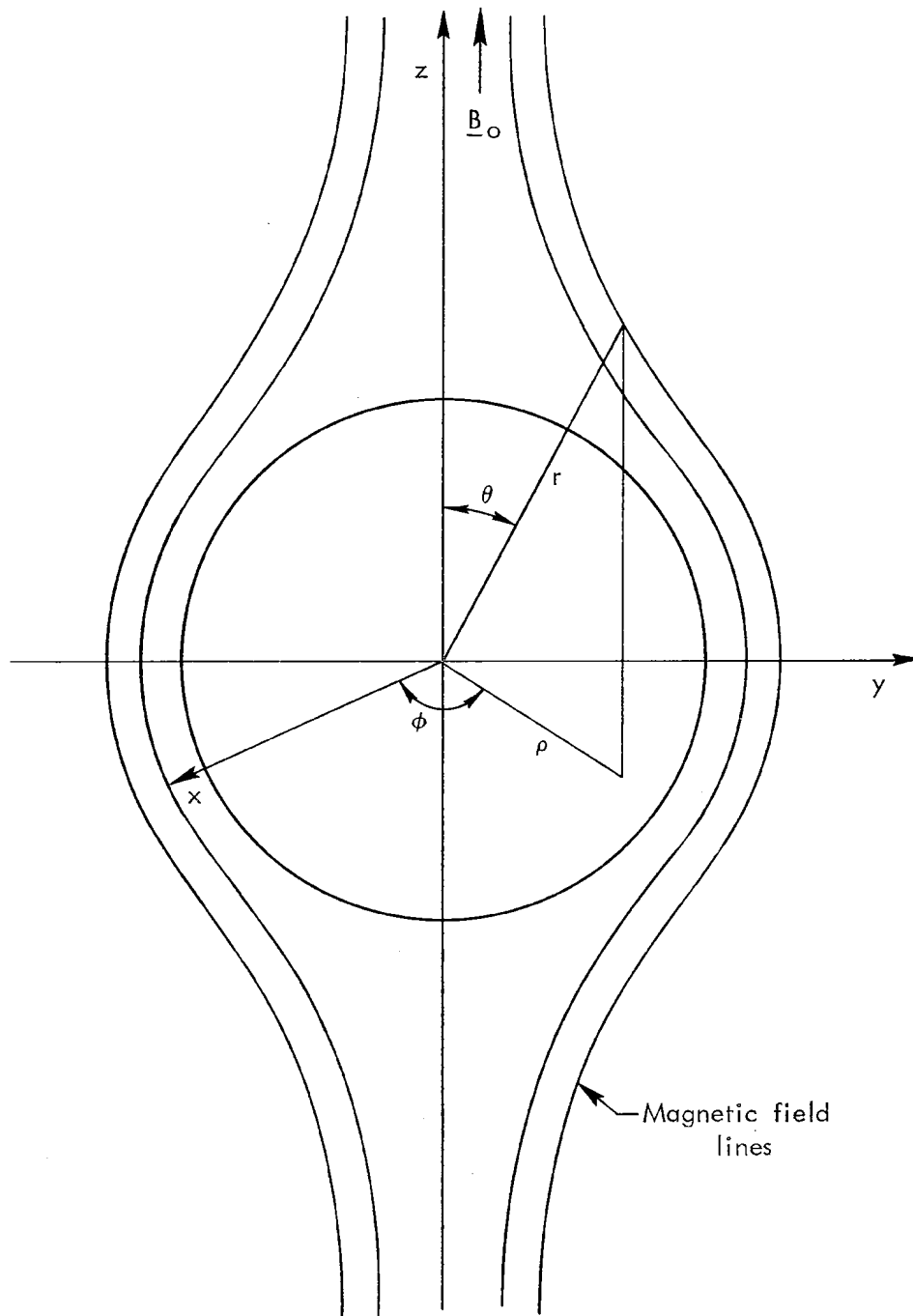


Fig.1—Cylindrical and spherical coordinate systems with origin at the center of the conductor and z axis parallel to \underline{B}_0

(slow) mode only to order $(\omega/\Omega_i)^2$, while the reverse is true to order ω/Ω_i . \tilde{E}_φ may therefore be found for $\tilde{E}_\rho = 0$, and then used as a source term for the anisotropic mode. The medium remains nondispersive through first order in ω/Ω_i , and both modes will propagate at the Alfven velocity. The zero- and first-order equations are

$$(\nabla \times \nabla \times \underline{\tilde{E}})_\varphi - \frac{\omega^2}{S^2} \tilde{E}_\varphi = 0 \quad (5a)$$

and

$$\frac{\partial^2 \tilde{E}_\rho}{\partial z^2} + \frac{\omega^2}{S^2} \tilde{E}_\rho = \frac{i\omega}{\Omega_i} \frac{\omega^2}{S^2} \tilde{E}_\varphi \quad (5b)$$

respectively, where it is assumed that $c^2/S^2 \gg 1$.

The boundary conditions at the surface are⁽¹⁴⁾

$$\underline{e}_r \cdot \underline{B} = 0 \quad (6a)$$

$$\underline{e}_r \times [\underline{E} + \underline{V} \times \underline{B}] = 0 \quad (6b)$$

where \underline{e}_r is the unit radial vector and $\underline{V} = V\underline{e}_r$ is the expansion velocity of the surface of the sphere. Equation (6a) implies that the magnetic field is always tangential at the surface. It will be shown from Eq. (6b) that the tangential electric field at the surface is $-\underline{V} \times \underline{B}$ when the sphere is moving, and zero after it stops. The electric field therefore "jumps" at the surface at $t = 0$ when the sphere begins to expand and at $t = \tau$ after it stops. The discontinuity in the zero-order electric field E_φ at any point in the non-dispersive medium will be, at most, a jump discontinuity, and hence the zero-order vector potential will be continuous.

For the given model, Eq. (5a) is solved for E_{φ} (and its Fourier transform \tilde{E}_{φ}) as a function of position in Appendix A, and E_{ρ} is calculated in Appendix B. The results are presented in Sections IV and V.

IV. THE ZERO-ORDER FIELDS

The zero-order vector potential is derived in Appendix A.

Defining $\eta = t - r/S$, and with $\beta = V/S$, the following electromagnetic fields are obtained:

$$B_r^I = B_o \cos \theta \left\{ 1 - \frac{\beta^3}{(1-\beta)^2(1+2\beta)} \left[\left(\frac{\eta S}{r} \right)^3 + 3 \left(\frac{\eta S}{r} \right)^2 \right] \right\} \quad (7a)$$

$$B_\theta^I = -\frac{1}{2} B_o \sin \theta \left\{ 2 + \frac{\beta^3}{(1-\beta)^2(1+2\beta)} \left[\left(\frac{\eta S}{r} \right)^3 + 3 \left(\frac{\eta S}{r} \right)^2 + 6 \left(\frac{\eta S}{r} \right) \right] \right\} \quad (7b)$$

$$E_\varphi^I = \frac{3}{2} \frac{B_o S \beta^3 \sin \theta}{(1-\beta)^2(1+2\beta)} \left[\left(\frac{\eta S}{r} \right)^2 + 2 \left(\frac{\eta S}{r} \right) \right] \quad (7c)$$

for

$$0 < \eta < (1-\beta)\tau$$

and

$$B_r^{II} = B_o \cos \theta \left\{ 1 - \frac{a^3}{r^3} + \frac{3\beta}{1+2\beta} \left(\frac{a^3}{r^3} - \frac{a^2}{r^2} \right) e^{-\left[\frac{\eta - (1-\beta)\tau}{\beta\tau} \right]} \right\} \quad (8a)$$

$$B_\theta^{II} = -B_o \sin \theta \left\{ 1 + \frac{a^3}{2r^3} + \frac{3}{2} \frac{\beta}{1+2\beta} \left(\frac{a^3}{r^3} + \frac{a^2}{r^2} - \frac{a}{r} \right) e^{-\left[\frac{\eta - (1-\beta)\tau}{\beta\tau} \right]} \right\} \quad (8b)$$

$$E_\varphi^{II} = \frac{3}{2} B_o \frac{\beta S}{1+2\beta} \sin \theta \left(\frac{a^2}{r^2} - \frac{a}{r} \right) e^{-\left[\frac{\eta - (1-\beta)\tau}{\beta\tau} \right]} \quad (8c)$$

for

$$\eta > (1-\beta)\tau.$$

The spatial dependence of the wave fields is similar to that of an oscillating magnetic dipole. At distances much greater than $\left(\frac{1-\beta}{\beta}\right)a$, only the $1/r$, or radiation, terms of the wave fields are of significance. The total zero-order induced fields are plotted versus time in Figs. 2-4. The magnitude of the induced fields increases with retarded time until the sphere stops expanding, and then the fields decay, with time constant $\beta\tau$, to those of a static magnetic dipole. During expansion, the tangential magnetic field at the surface $\left(\eta = \left(\frac{1-\beta}{\beta}\right) \frac{r}{S}\right)$ is constant and equal to

$$B_{\theta s}^I = -\frac{3}{2} B_o \frac{(1+\beta)}{(1-\beta)(1+2\beta)} \sin \theta \quad (9a)$$

and

$$E_{\phi s}^I = -\beta S B_{\theta s} \quad (9b)$$

For $t > \tau$, the surface fields (i.e., $\eta = t - a/S$) are given by

$$B_{\theta s}^{II} = -\frac{3}{2} B_o \sin \theta \left[1 - \frac{\beta}{1+2\beta} e^{-\left(\frac{t-\tau}{\beta\tau}\right)} \right] \quad (10)$$

with $E_{\phi s}^{II} = 0$. The surface current density $j_s \frac{e}{\phi}$, correct to terms of order V^2/c^2 , is equal to $B_{\theta s}/\mu_o$, where c is the vacuum speed of light, and $\mu_o = 4\pi \times 10^{-7}$ MKS units. In Fig. 5, j_s is plotted as a function of time. The surface current density remains constant in time during expansion, then "jumps" at the instant the electric field at the surface vanishes, and finally decays to just that value needed to expel the geomagnetic field from the conductor.

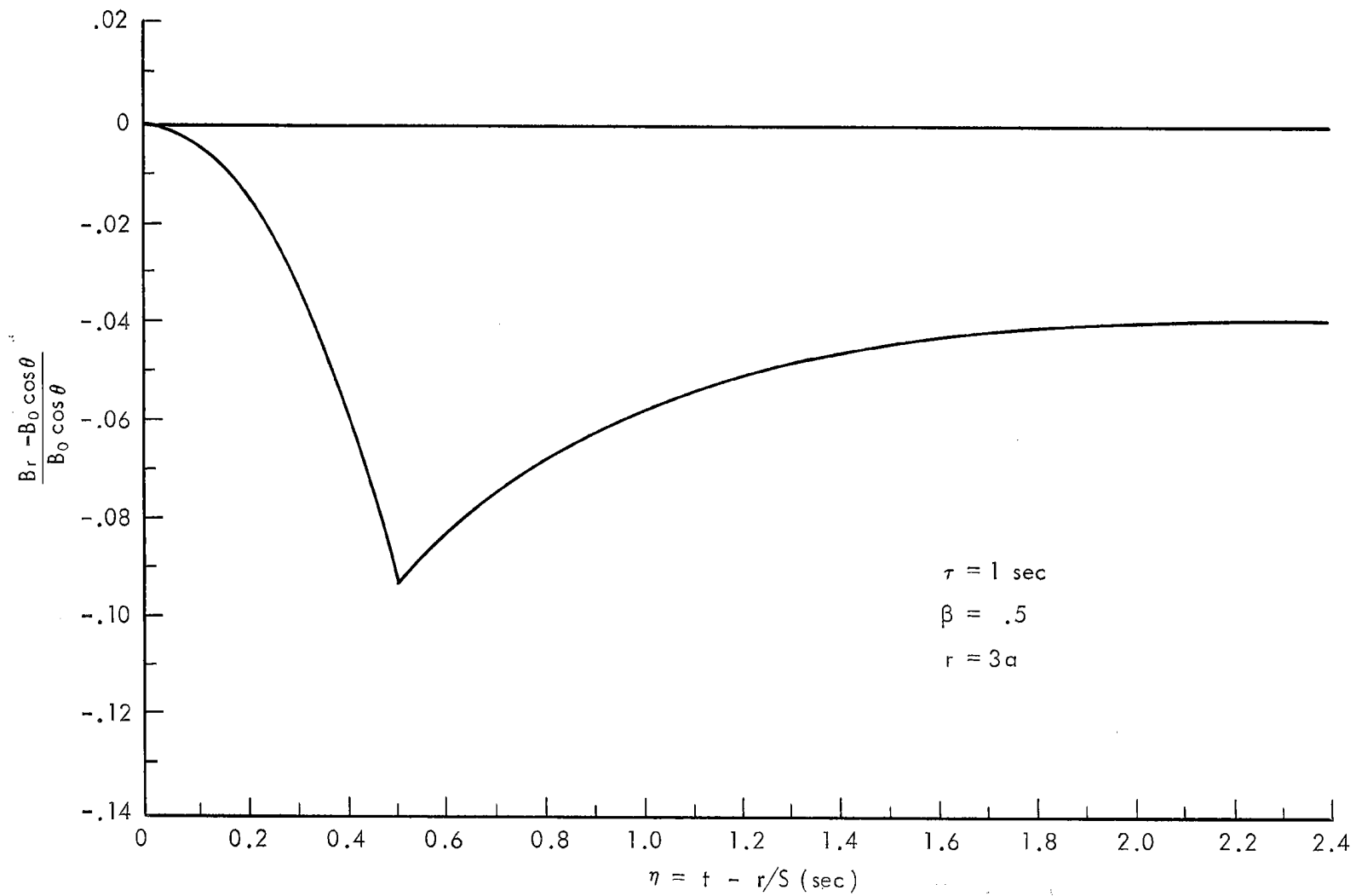


Fig.2—The radial component of induced magnetic field versus retarded time $\eta = t - r/S$

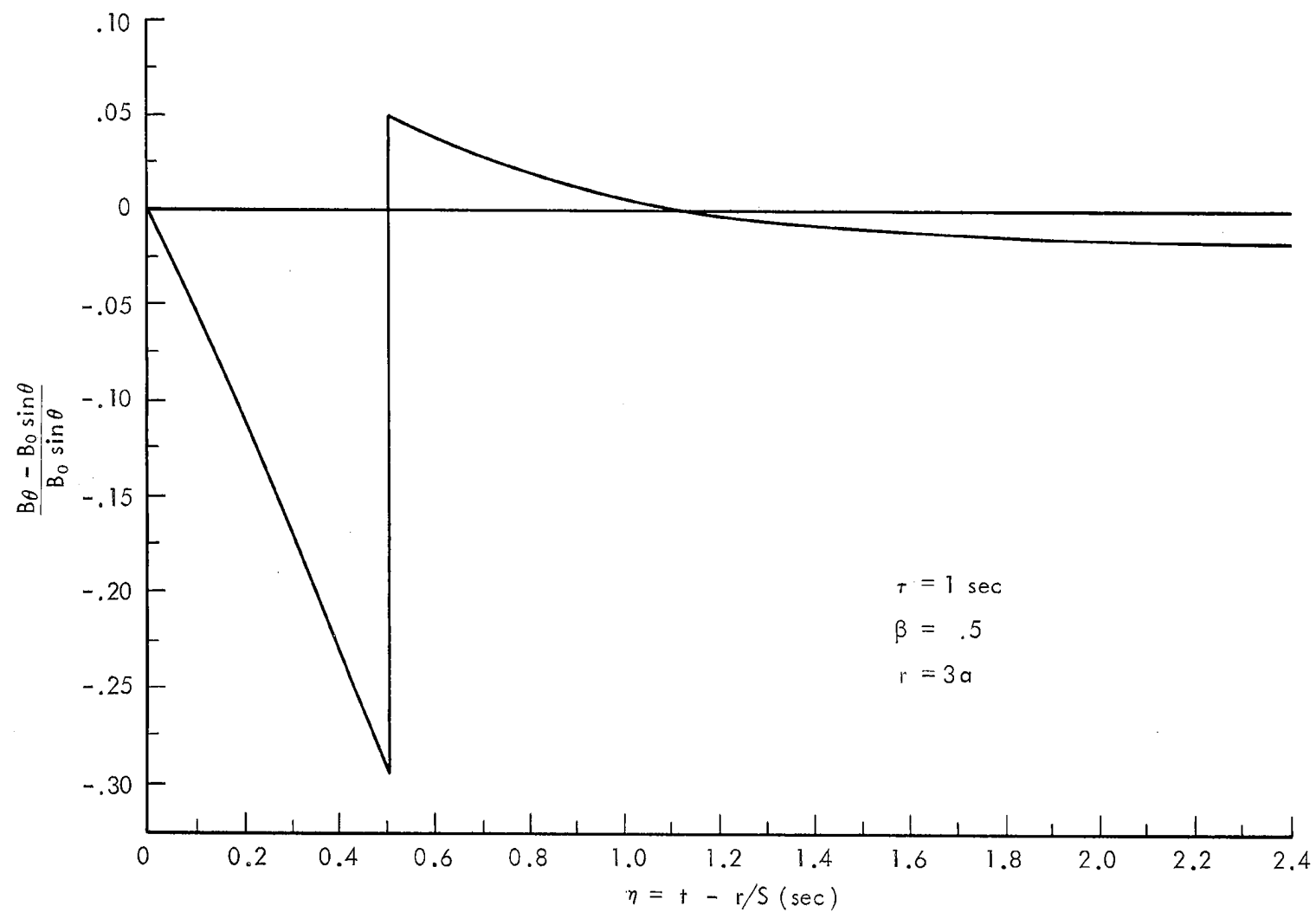


Fig.3—The θ component of induced magnetic field versus η

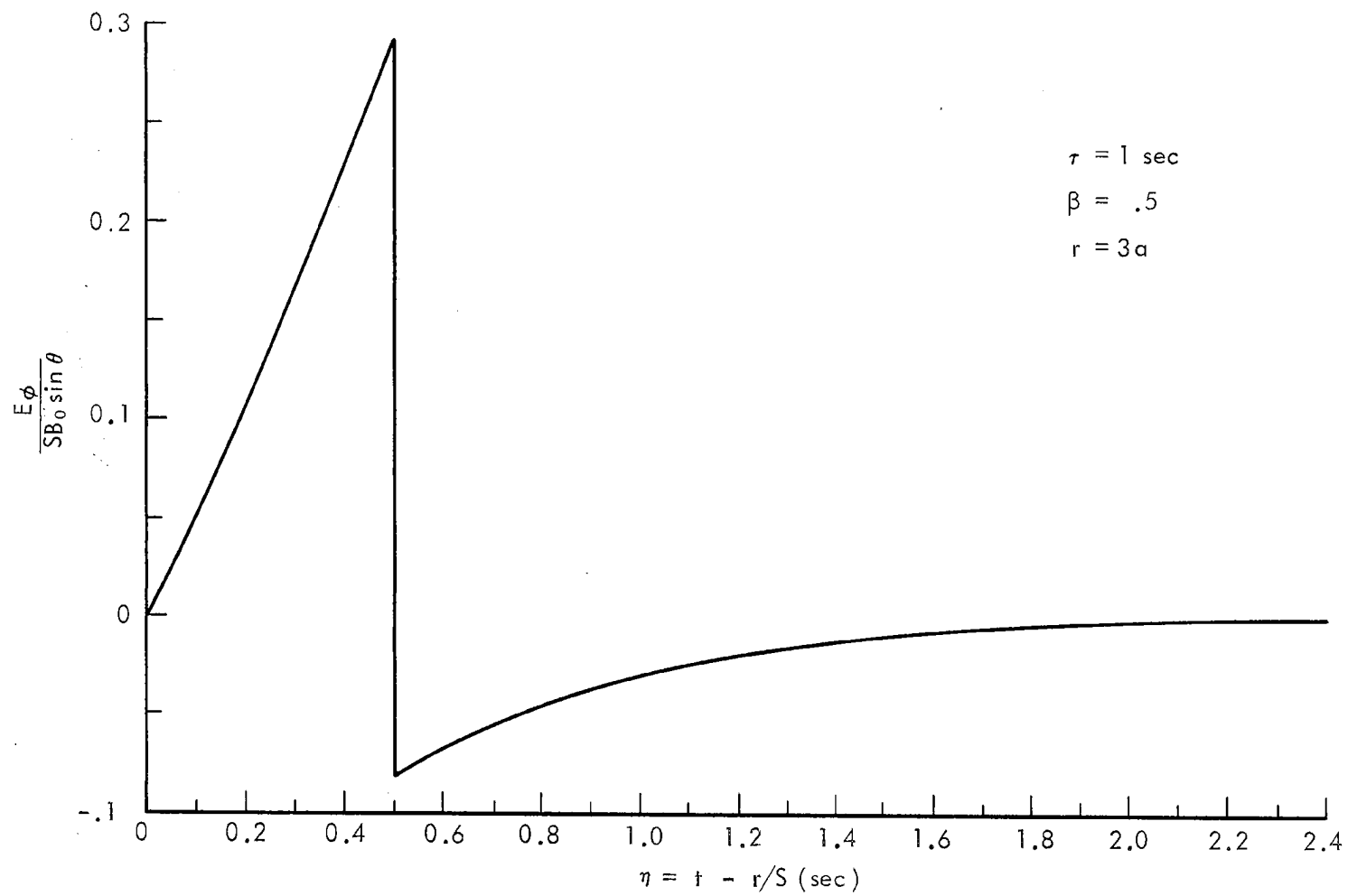


Fig.4—The induced electric field E_ϕ versus η

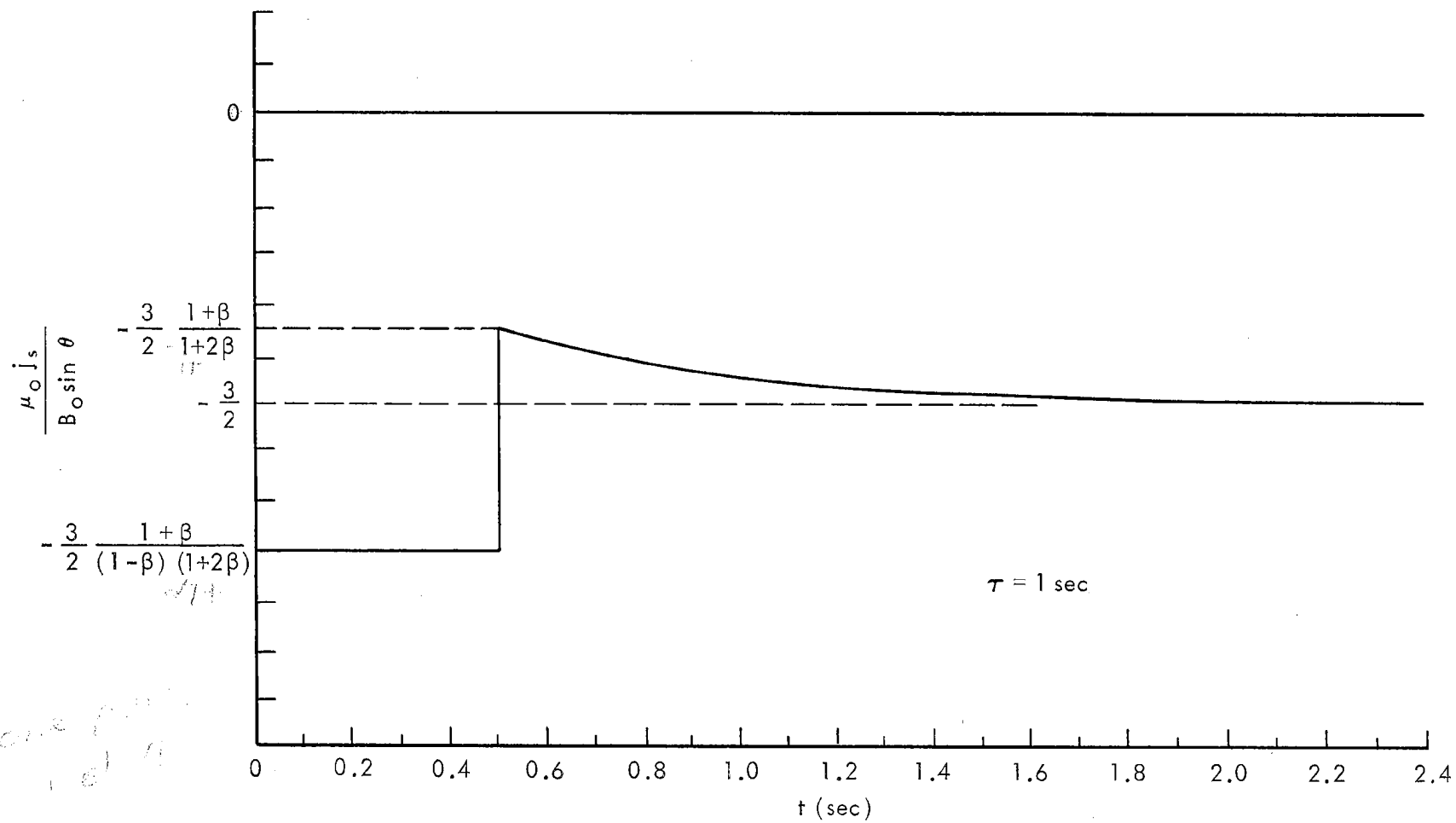


Fig.5—Surface current density j_s versus time t

The Fourier decomposition of the fields is also of interest for problems involving the transmission of these signals through a dispersive medium, e.g., the ionosphere. Then \tilde{E}_φ , the Fourier transform of E_φ , is given by

$$\tilde{E}_\varphi = \int_{r/S}^{\infty} E_\varphi(r, \theta, t) e^{i\omega t} dt = e^{ikr} \int_0^{\infty} E_\varphi(r, \theta, \eta) e^{i\omega\eta} d\eta \quad (11)$$

where $k = \omega/S$. Carrying out the integration yields

$$\tilde{E}_\varphi = H(\omega) e^{ikr} \left[\frac{1}{r} - \frac{ik}{r} \right] \sin \theta \quad (12)$$

where

$$H(\omega) = \frac{3}{2} \frac{B_o a^3}{(1+2\beta)(i\omega\tau)} e^{2ix} \left[\frac{1}{1-i\beta\omega\tau} + \frac{1}{ix} \left(e^{-ix} \frac{\sin x}{x} - 1 \right) \right]$$

and

$$x = \frac{1}{2} \omega(1-\beta)\tau.$$

For $|\omega\tau| \ll 1$, $H(\omega) \rightarrow \frac{1}{2} B_o a^3$, and

$$\tilde{E}_\varphi \rightarrow \frac{1}{2} B_o a^3 \left(\frac{1}{r} - \frac{ik}{r} \right) \sin \theta e^{ikr} \quad (13)$$

The transform for $|\omega| \ll 1/\tau$ approaches that of an instantaneously created dipole with moment $-2\pi B_o a^3/\mu_o$, and in this limit agrees with the solution obtained by Karplus.*

*See Ref. 13, p. 803.

V. ENERGY CONSIDERATIONS AND RADIATION

It is of interest to determine the hydromagnetic energy radiated from the model as a function of expansion velocity. Leipunskii⁽¹⁰⁾ has estimated that

$$V \sim \left(\frac{Y_H}{M} \right)^{\frac{1}{2}} \quad (14)$$

where Y_H is the hydrodynamic yield of the device and M is the mass of the ionized bomb products. Assuming V remains constant, the total energy required to expand the conductor is calculated in this section as a function of its final radius, and is equated to Y_H . One can then estimate the radius a and expansion time τ for a given yield. The energy radiated into MHD waves is also calculated, and by normalizing to a given yield Y_H , the efficiency of the system as a radiator of hydromagnetic waves can be defined. A discussion of the interaction energy between the sphere and the field is presented here, and conservation of energy is demonstrated.

It is first observed that it is sufficient to retain only the zero-order fields in computing the energy through first order in (ω/Ω_i) . Then, consider the radial component of the Poynting vector for the zero-order fields $\underline{P} = \frac{1}{\mu_o} \underline{E} \times \underline{B}$, noting those terms which do not vanish when integrated over an infinite sphere, i.e., which fall off no faster than $1/r^2$. These terms are

$$P^I = \frac{3}{2} \frac{B_o^2}{\mu_o} \frac{S\beta^3}{(1-\beta)^2(1+2\beta)} \sin^2 \theta \left[2 \left(\frac{\eta S}{r} \right) + \left(\frac{\eta S}{r} \right)^2 + 6 \left(\frac{\eta S}{r} \right)^2 \right] \quad (15a)$$

for $0 < \eta < (1-\beta)\tau$, and

$$P^{II} = \frac{3}{2} \frac{B_o^2}{\mu_o} \frac{S\beta}{(1+2\beta)} e^{-\left(\frac{\eta-(1-\beta)\tau}{\beta\tau}\right)} \sin^2 \theta \left[-\frac{a}{r} + \frac{a^2}{r^2} - \frac{3}{2} \frac{\beta}{1+2\beta} \frac{a^2}{r^2} e^{-\left(\frac{\eta-(1-\beta)\tau}{\beta\tau}\right)} \right] \quad (15b)$$

for $\eta > (1-\beta)\tau$. The total energy W_T passing through a large sphere of radius R is then given by

$$W_T = \int_0^{2\pi} d\phi \int_0^\pi d\theta \sin \theta R^2 \left[\int_0^{(1-\beta)\tau} d\eta P^I(r=R) + \int_{(1-\beta)\tau}^\infty d\eta P^{II}(r=R) \right] \quad (16)$$

It is instructive to integrate and discuss separately the three terms in each of the brackets in Eq. (15) since the associated energies have different physical interpretations. The last term in each of the brackets of Eq. (15a) and Eq. (15b) arises from taking the vector product of the radiation $(1/r)$ electric and magnetic fields and represents true hydromagnetic radiation. Carrying out the integration over these terms yields

$$W_R = \frac{\pi B_o^2 a^3}{\mu_o} \frac{\beta^2 (3+5\beta)}{(1-\beta)(1+2\beta)^2} \quad (17)$$

for the hydromagnetic wave energy, W_R .

The first two terms in each of the brackets in Eqs. (15a) and (15b) arise from taking the vector product of the electric field with the static magnetic field, $B_o \underline{e}_z$. First performing the η integration over the $1/r$ terms shows that the contributions from P^I and P^{II} exactly cancel. Hence, the $1/r$ terms in P^I and P^{II} represent energy which flows from the sphere during expansion and then returns to it without ever being lost from the system.

The integration over the second term in the brackets yields a finite contribution to the energy, which will temporarily be designated by W_S , and is equal to

$$W_S = \frac{4}{3} \frac{\pi B_o^2 a^3}{\mu_o} \quad (18)$$

which is noted to be independent of β . The total integrated Poynting vector is thus $W_S + W_R$, but W_S is not associated with hydromagnetic radiation.

The physical significance of W_S will be more readily understood after calculating W_B , the apparent change in energy stored in the magnetic field due to the presence of the sphere. The magnetic energy density is $(B_r^2 + B_\theta^2)/2\mu_o$, and the value of \underline{B} at $t = \infty$ is equal to

$$B_\infty = B_o \left[\cos \theta (1 - a^3/r^3) \underline{e}_r - \sin \theta (1 + 2a^3/r^3) \underline{e}_\theta \right] \quad (19)$$

for $r > a$, and zero for $r < a$. Integrating $(1/2\mu_o) [B_\infty^2 - B_o^2]$ over all space, and defining the result to be W_B yields

$$W_B = - \frac{\pi B_o^2 a^3}{3\mu_o} = \frac{1}{6} \underline{M} \cdot \underline{B}_o \quad (20)$$

where $\underline{M} = - 2\pi B_o a^3/\mu_o$ is the dipole moment of the sphere. Now the interaction energy between the field and the conductor is mathematically identical to that between the field and a uniformly magnetized sphere of magnetization $m = M/(\frac{4}{3} \pi a^3)$. However, the total interaction energy of a magnetized body in a uniform magnetic field B_o produced

by fixed currents is well known to be ⁽¹⁵⁾ $W_I = -\frac{1}{2} \underline{M} \cdot \underline{B}_O$, where M is the total magnetic moment of the body. Hence, the real interaction energy is

$$W_I = -\frac{1}{2} \underline{M} \cdot \underline{B}_O = \frac{\pi B_O^2 a^3}{\mu_O} \quad (21)$$

which is precisely $W_S + W_B$. The difference in interpretation between Eqs. (20) and (21) has been discussed in detail by Gilinsky and Holliday.⁽¹⁶⁾ They have shown that in order to obtain the correct energy (Eq. (21)), it is necessary to compute the interaction between the sphere and a finite source of magnetic field, and to take the limit of a uniform field correctly. The total interaction energy is then $W_S + W_B$, where W_B can be interpreted as only a local change in magnetic field energy. In order to discuss where W_S "goes," it is necessary to assume a model for the source of the earth's magnetic field. Any model, however, can be reduced to linear combinations of two cases: a current "loop" producing constant magnetic flux, and a loop with constant current. In the first case, W_S as well as W_B will appear as stored magnetic energy. In the constant current case, the changing flux through the loop will induce an EMF, and there will be a net energy change in the source (e.g., a battery) producing the current in the loop. In this case, it can be shown that in general

$$\Delta W_{\text{battery}} = -2\Delta W_{\text{field}}$$

Therefore, $\Delta W_{\text{battery}} = - \underline{M} \cdot \underline{B}_0 = + 2\pi B_0^2 a^3 / \mu_0$, and the total change in field energy is $+ \frac{1}{2} \underline{M} \cdot \underline{B}_0 = - \pi B_0^2 a^3 / \mu_0$. In either of these two cases, the total interaction energy is $- \frac{1}{2} \underline{M} \cdot \underline{B}_0 = W_S + W_B$.

A number of authors have estimated the expansion radius by equating Y_H to the magnitude of W_B , the local field energy displaced by the conducting sphere. This gives a correct order of magnitude only because all of the energy changes scale as $B_0^2 a^3 / \mu_0$; however, the physical reasoning is incorrect. Y_H should actually be equated to the total work done in expanding the sphere to radius a , which can be calculated by conservation of energy:

$$Y_H = W_R + W_S + W_B = \frac{\pi B_0^2 a^3}{\mu_0} \frac{(1+\beta)^2}{(1+2\beta)^2(1-\beta)} \quad (22)$$

In the limit $\beta \rightarrow 0$, in which there is negligible radiation, Y_H is then given by the total interaction energy, and not $|W_B|$. The work may also be computed by integrating the Maxwell stresses over the surface of the sphere. This calculation is carried out in Appendix B, and the result is shown to agree with Eq. (22).

Assuming that Y_H and B_0 are known, the variation of a with β (e.g., varying the mass M) can be calculated. In Fig. 6, $\left(\pi B_0^2 / \mu_0 Y_H\right)^{1/3} a$ versus β is plotted. The fact that the expansion radius a decreases with increasing β implies that there is more radiation, and work is thus expended at a faster rate at higher expansion velocities. In Fig. 7, $S \left(\pi B_0^2 / \mu_0 Y_H\right)^{1/3} \tau$ is plotted as a function of β . The expansion time τ varies as $1/\beta$ for small β , and decreases more rapidly for larger β . The curves are broken for β close to 1 because

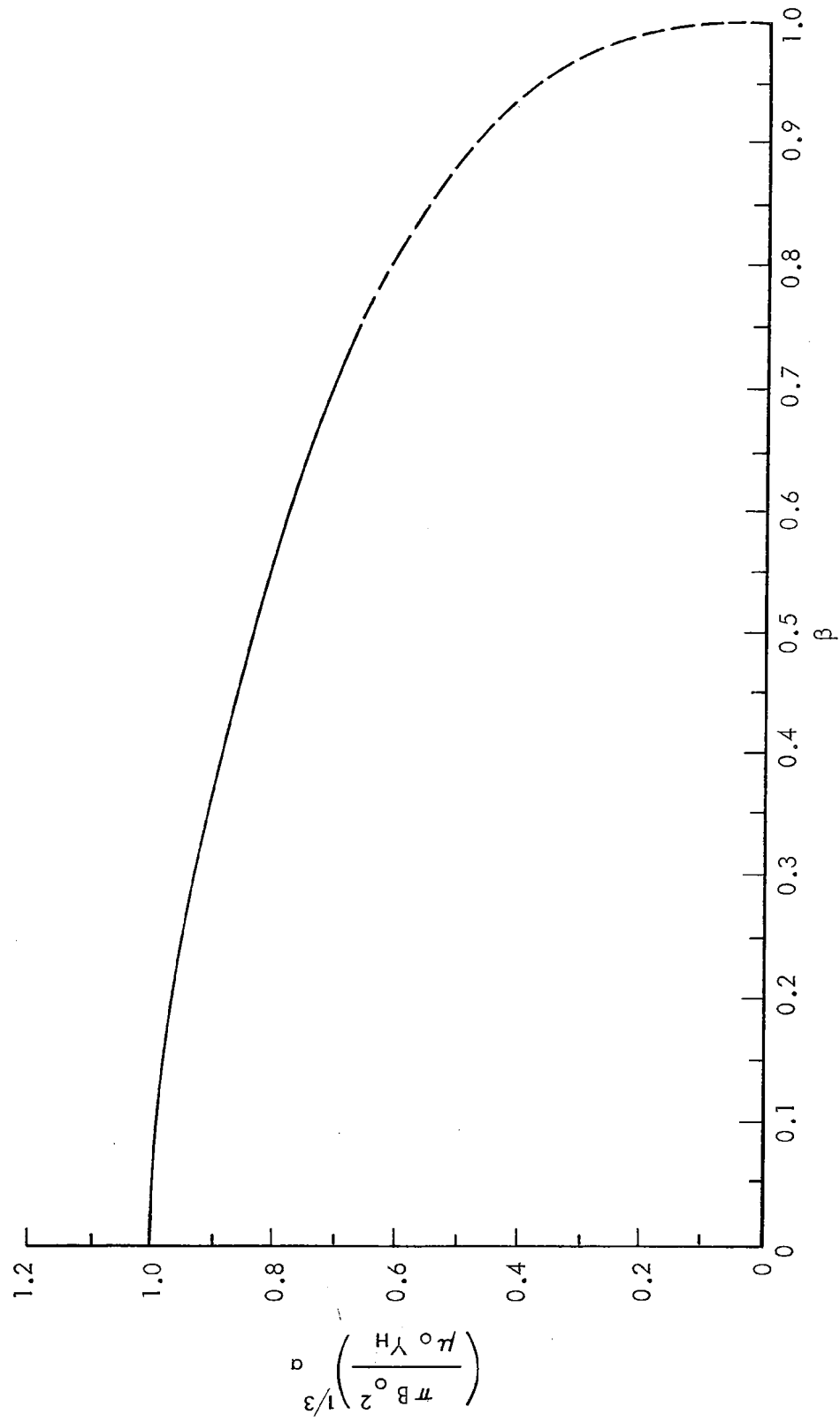


Fig. 6—Expansion radius a versus β for a fixed hydromagnetic yield Y_H

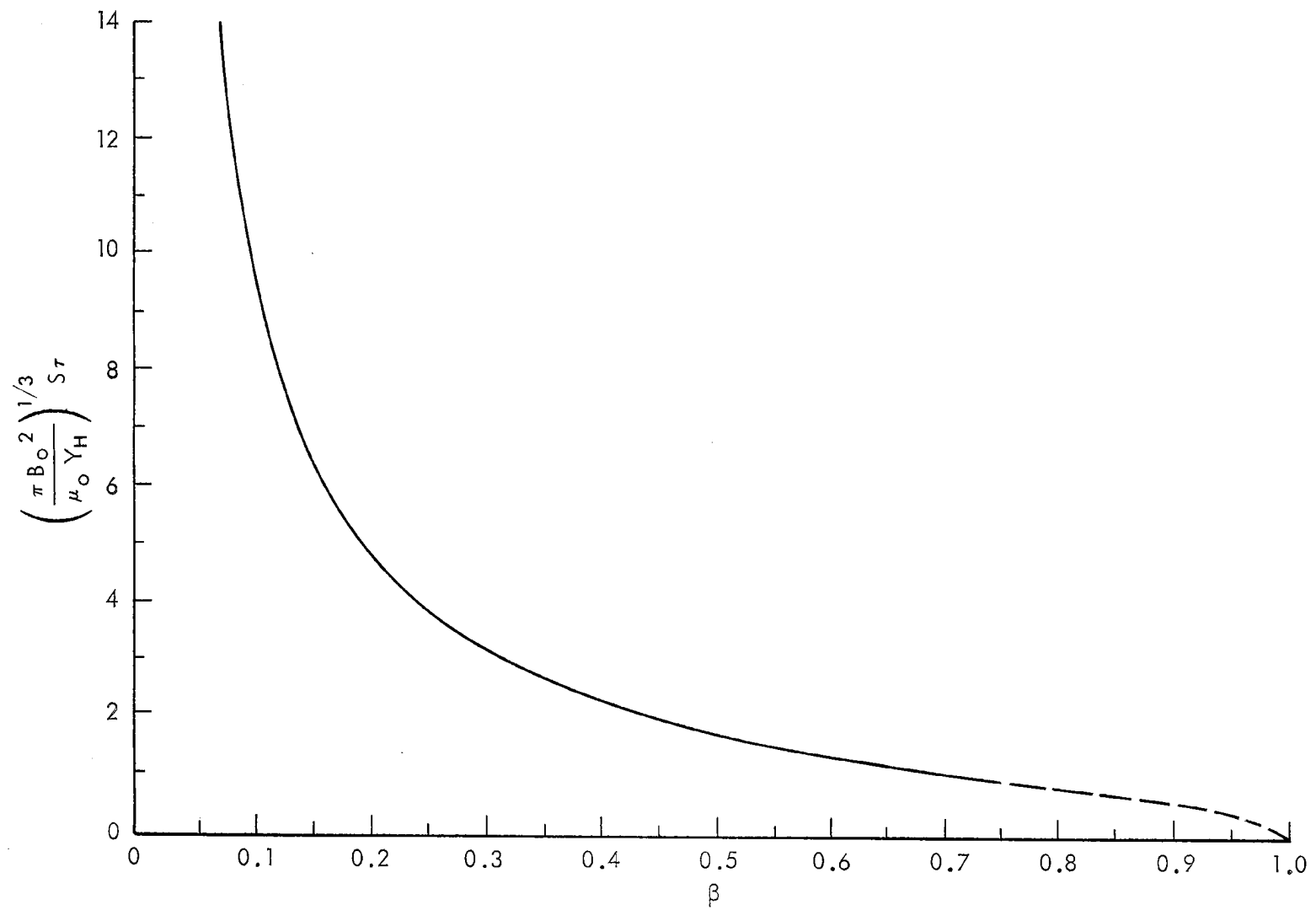


Fig.7—Expansion time τ versus β for a fixed hydromagnetic yield Y_H

in this region the use of linearized theory for the conductivity is not justified.

The ratio

$$\frac{W_R}{Y_H} = \frac{\beta^2 (3+5\beta)}{(1+\beta)^3} \quad (23)$$

is the fraction of energy radiated into hydromagnetic waves for a given yield Y_H , which is the radiation efficiency of the system and is plotted in Fig. 8. For $\beta \ll 1$, a very small fraction of Y_H appears as radiation, while for β close to 1, almost all of the yield goes into wave energy. Therefore, this model predicts that for very-high-altitude bursts where the ground level signal is determined predominately by the radiation field, much larger hydromagnetic signals would be produced from bursts with higher expansion velocities (i.e., smaller masses) for a given Y_H .

To compute the power spectral density, the relation $E_\varphi = -SB_\theta$ for the radiation fields can be utilized, and $|\tilde{E}_\varphi|^2/2\pi S\mu_0$ can be computed from Eq. (12). Expressing the result in terms of Y_H yields for $W_R(\omega)$, the spectrum of the energy radiated into the solid angle $d\Omega = \sin \theta d\theta d\varphi$:

$$W_R(\omega) = \left(\frac{\mu_0 Y_H^4}{B_0^2} \right)^{1/3} \frac{9 \sin^2 \theta}{8\pi^{7/3} S(1+\beta)^4} \frac{[(1+2\beta)^2 (1-\beta)^4]^{1/3}}{x^2} \left\{ 1 + \left(\frac{\sin x}{x} \right)^2 + \frac{(1+2\alpha)x^2}{1 + (\alpha x)^2} - 2 \sin x \left[\frac{\cos x}{x} + \frac{\alpha x \cos x + \sin x}{1 + (\alpha x)^2} \right] \right\} \quad (24)$$

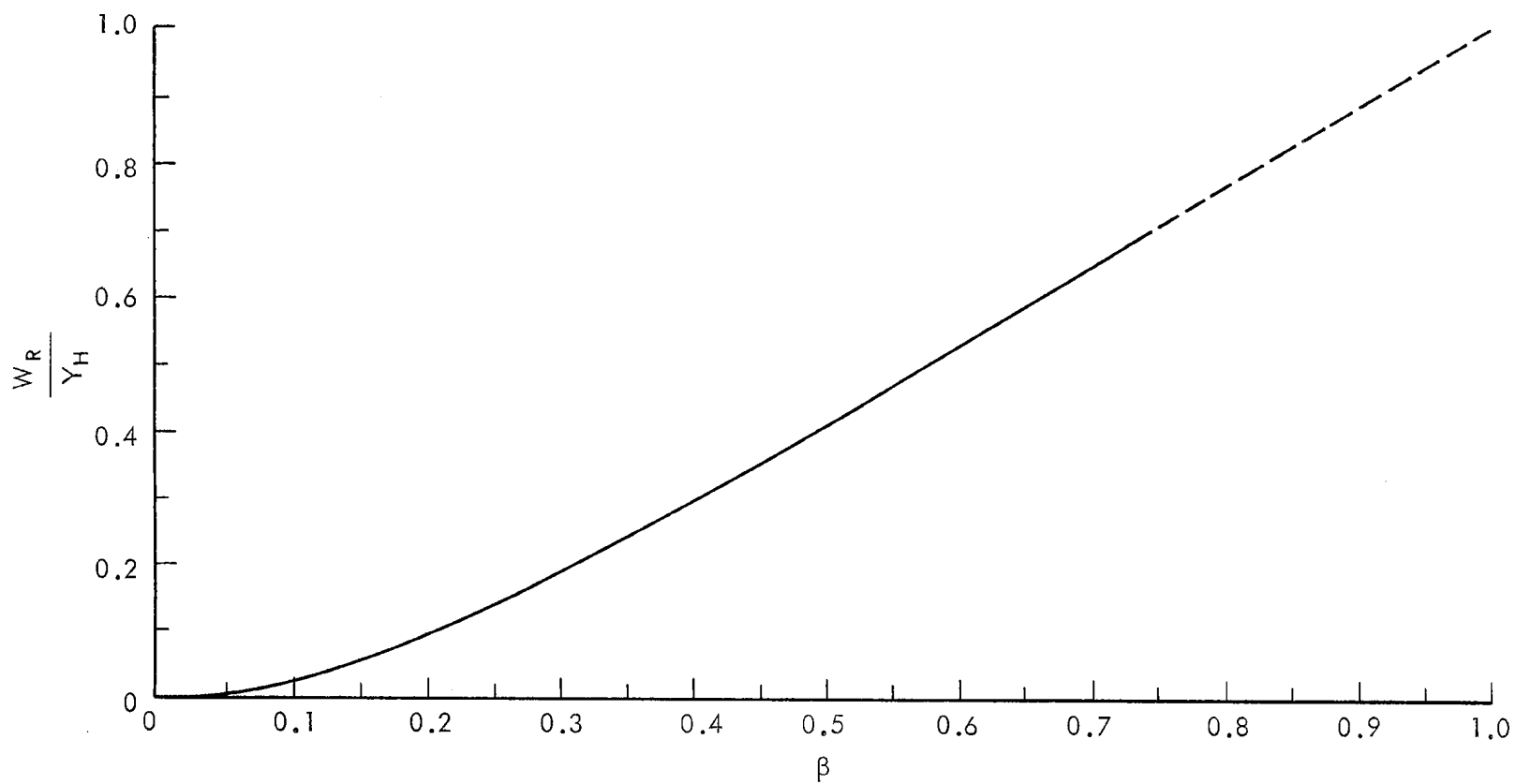


Fig.8—Radiation efficiency W_R / Y_H versus β for a fixed hydromagnetic yield Y_H

where $\alpha = 2\beta/(1-\beta)$. $W_R(\omega)$ versus $\omega\tau$ is shown in Fig. 9 for $\beta = .1, .5$, and $.9$. $W_R(\omega)$ increases as ω^2 for small ω , decreases as $1/\omega^2$ for large ω , and peaks at $\omega\tau \approx 4$ or at $f \approx .6\tau^{-1}$, with the spectra becoming flatter in the vicinity of the peak as $\beta \rightarrow 1$. For $\omega\tau \lesssim 1$ (see Eq. (13)),

$$W_R(\omega) \rightarrow \frac{B_o^2 a^6 \omega^2}{8\pi\mu_o S^3} \sin^2 \theta = \frac{1}{8\pi^3} \frac{\mu_o Y_H^2}{B_o^2 S^3} \left[\frac{(1+2\beta)^2 (1-\beta)}{(1+\beta)^3} \right]^2 \omega^2 \sin^2 \theta \quad (25)$$

It is of interest to compute the total energy radiated in the frequency band from zero to some frequency $\omega_f (\ll 4/\tau)$ for applications where band-limited equipment is utilized. Integrating Eq. (24) over frequencies and solid angle yields

$$\begin{aligned} W_f &= \int_{-\omega_f}^{\omega_f} d\omega \int W_R(\omega) d\Omega = \frac{2}{9\pi^2} \frac{\mu_o Y_H^2}{B_o^2 S^3} \left[\frac{(1+2\beta)^2 (1-\beta)}{(1+\beta)^3} \right]^2 \omega_f^3 \\ &= \frac{2}{9\pi} \left(\frac{\beta}{1+\beta} \right)^3 (1+2\beta)^2 (1-\beta) (\omega_f \tau)^3 Y_H \quad (26) \end{aligned}$$

A few examples are now presented to illustrate the applications of the above theory.

EXAMPLE 1

Leipunskii⁽¹⁰⁾ has estimated the plasma mass M of Argus to be ~ 500 kg. Taking $Y_H = 1 \text{ KT} = 4.2 \times 10^{12} \text{ J}$, the expansion velocity $V \sim \sqrt{Y_H/M} = 91 \text{ km/sec}$. Then, if an Argus type burst were exploded in the daytime at an altitude of 480 km, $S \approx 250 \text{ km/sec}$ and $\beta \approx .36$. Assuming $B_o = 5 \times 10^{-5} \text{ W/m}^2$, Eq. (22) gives for the expansion radius $a = 80 \text{ km}$. The expansion time $\tau = a/V = .88 \text{ sec}$. The radiation

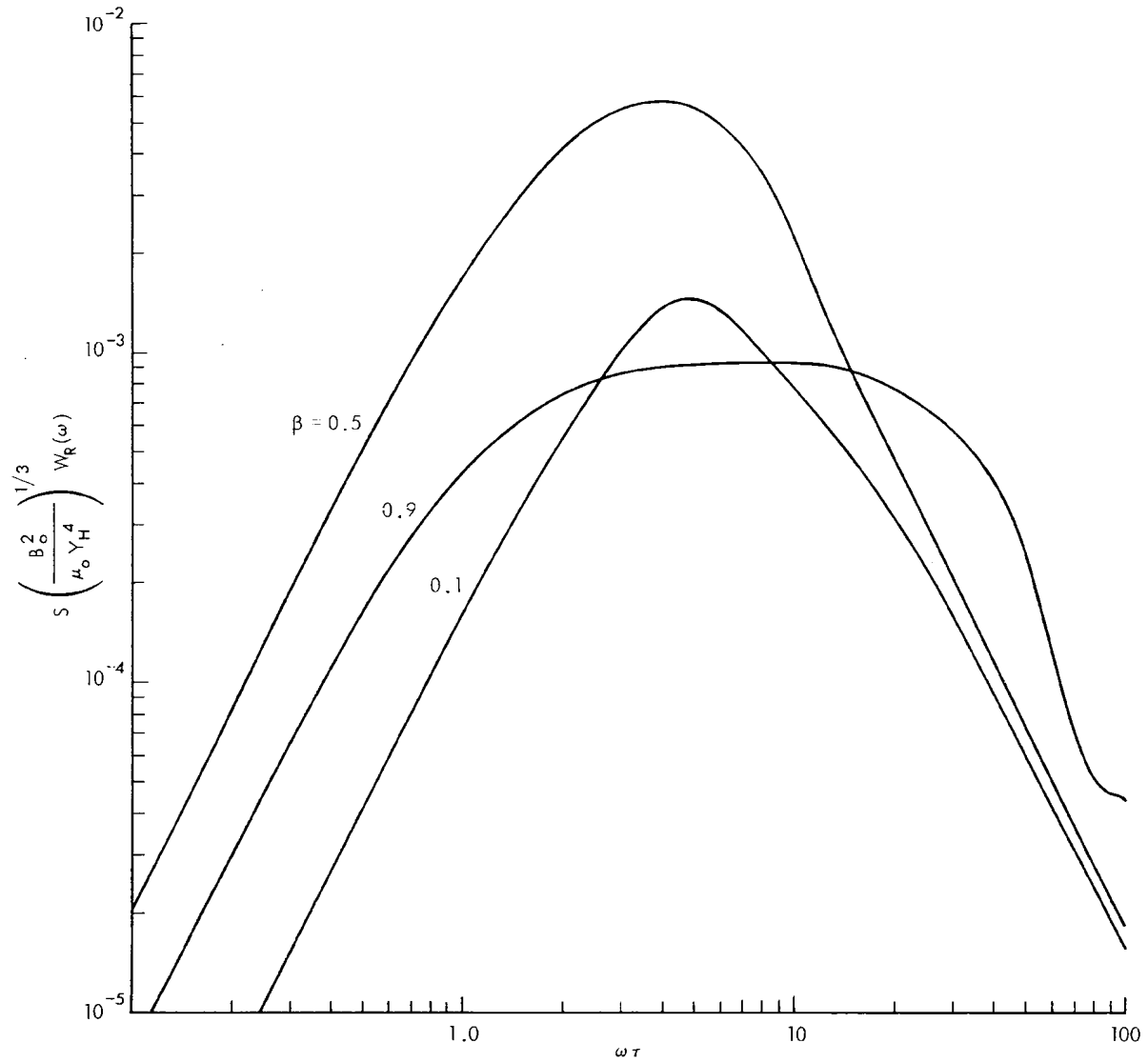


Fig.9—Frequency spectrum of hydromagnetic radiation
 $W_R(\omega)$ per solid angle versus $\omega \tau$

efficiency W_R/Y_H from Fig. 7 is .25, and therefore $W_R = .25$ KT. From Eq. (26) the energy content of the spectrum from 0 to ω_f is $W_f = 1.7 \times 10^{-3} \omega_f^3$ KT ($\omega_f \ll 4 \text{ sec}^{-1}$).

EXAMPLE 2

Consider a bomb of the same yield and mass as in Example 1, but exploded at an altitude of 2000 km. Use the parameters $S = 4500 \text{ km/sec}$ and $B_0 = 5 \times 10^{-5} \text{ W/m}^2$. Then $\beta = .02$, the expansion radius $a = 87 \text{ km}$, and $\tau = .96 \text{ sec}$. The radiation efficiency is 1.2×10^{-3} , the MHD radiation $W_R = 1.2 \times 10^{-3} \text{ KT}$, and $W_f = .5 \cdot 10^{-6} \omega_f^3$ KT for $\omega_f \ll 4 \text{ sec}^{-1}$.

EXAMPLE 3

Lapp⁽¹⁸⁾ has used an estimate of 1 KT/lb, which implies an expansion velocity $V = 3 \times 10^3 \text{ km/sec}$. Consider an altitude of 2000 km, and $Y_H = 1 \text{ KT}$. Then $\beta = .66$, $a = 64 \text{ km}$, $\tau = .02 \text{ sec}$, $W_R/Y_H = .6$, $W_R = .6 \text{ KT}$, and $W_f = .6 \times 10^{-7} \omega_f^3$ KT for $\omega_f \ll 200 \text{ sec}^{-1}$.

Comparing Examples 1 and 2, the radiated MHD energy W_R for an Argus type burst is reduced for the higher altitude because of the smaller ratio of expansion velocity to local Alfven speed. In the first example, one-fourth of the hydromagnetic yield appears as radiation, while in the second, almost all of the energy is dissipated by quasi-statically creating the dipole. Increasing the yield-to-mass ratio, as in Example 3, increases W_R and also the frequency spread over which the radiation occurs.

Figure 10, for $V = 200 \text{ km/sec}$ ($Y_H/M \sim .005 \text{ KT/lb}$), plots the radiation efficiency W_R/Y_H versus altitude, using a nighttime sunspot minimum altitude profile for the Alfven speed.⁽³⁾ The two orders of

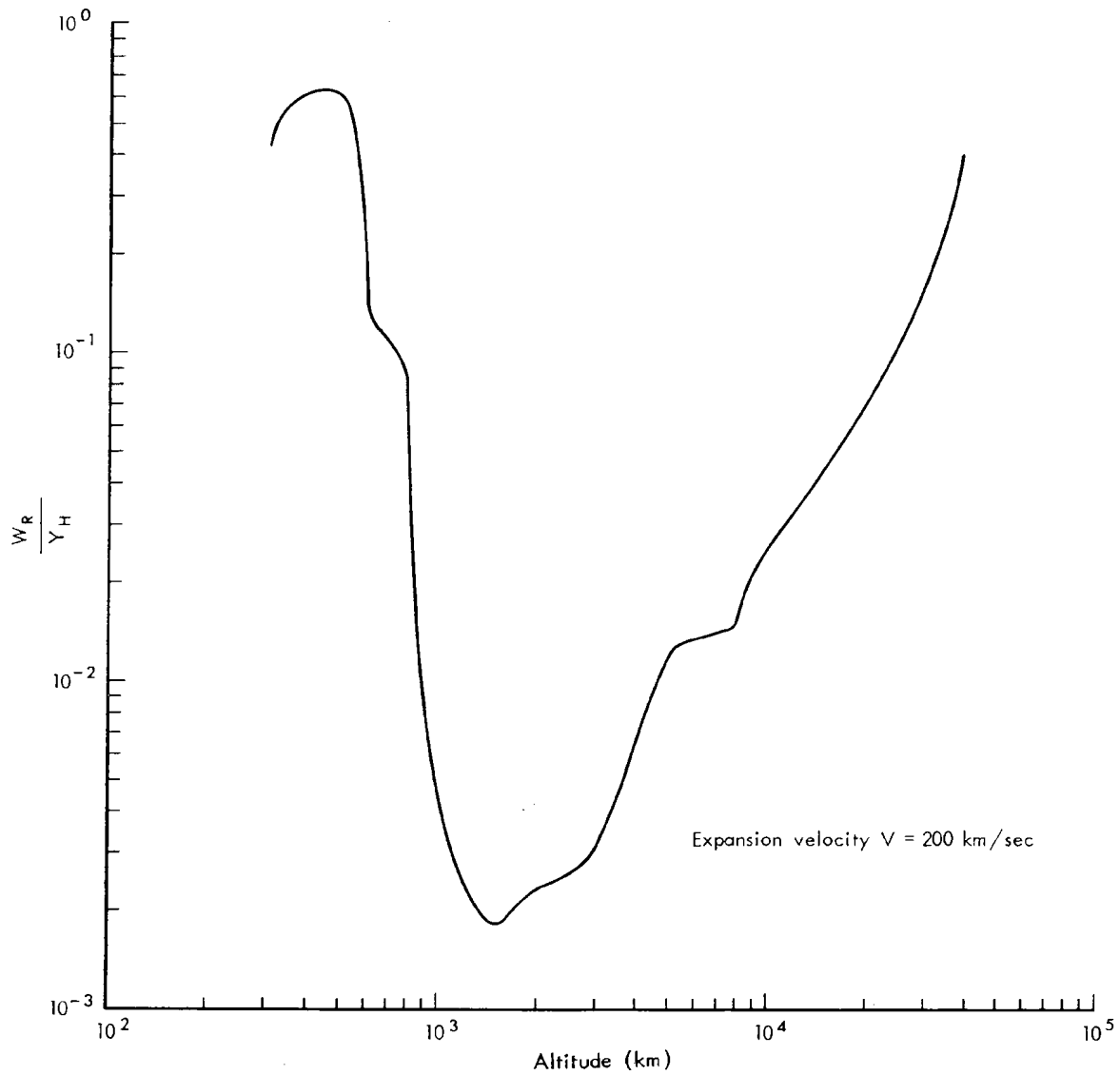


Fig. 10—Radiation efficiency W_R / Y_H versus altitude using a nighttime sunspot minimum altitude profile for the Alfvén speed

magnitude fluctuation in W_R/Y_H is due to the large variation in Alfvén speed with altitude. However, it must be stressed that the concept of radiation efficiency as defined here is useful only as it relates to the strength of the signal produced by the source, and not to ultimate detection, which also depends upon the propagation medium. The interpretation is further restricted to bursts having expansion radii less than the local scale height of the Alfvén speed at the altitude of detonation. Finally, for distances from the burst such that the inequality $r \gg a$ is not satisfied, it is necessary to consider all of the fields of Eqs. (7) and (8) as part of the signal.

VI. THE FIRST-ORDER AND TOTAL FIELDS

In this section, the generation of the slow or anisotropic mode is analyzed for the idealized model under consideration. E_φ , the solution found to the zero-order equation, Eq. (5a), is used as a source term for E_ρ in the first-order equation, Eq. (5b). Equation (5b) is solved for E_ρ in the time domain subject to the appropriate boundary conditions.

The inverse transform of Eq. (5b) is

$$\frac{\partial^2 E_\rho}{\partial z^2} - \frac{1}{s^2} \frac{\partial^2 E_\rho}{\partial t^2} = - \frac{1}{\Omega_i s^2} \frac{\partial^3 E_\varphi}{\partial t^3} \quad (27)$$

From Eq. (7c), the righthand side of Eq. (27) is zero for $0 < n < (1-\beta)\tau$. Therefore, to first order in (ω/Ω_i) , E_ρ is not excited at all until the sphere has stopped. The problem is then reduced to one involving time-independent boundary conditions. Equation (27), or its transform, Eq. (5b), is merely the differential equation governing the motion of a vibrating string with a distributed source term. Outside of a cylinder of radius $\rho = r \sin \theta = a$, the "string" is infinitely long. For $\rho \leq a$ the string is fixed (i.e., $E_\rho = 0$) at $z = d \equiv \sqrt{a^2 - \rho^2}$, and waves will be reflected from the surface.

Equation (5b) is solved in Appendix C, subject to the boundary conditions above plus the condition of outgoing waves at infinity, from the Green's function. The solution is

$$\tilde{E}_\rho = - \frac{\omega}{\Omega_i} k \frac{H(\omega) e^{ikr}}{\rho} \quad \rho > a \quad (28a)$$

$$= - \frac{\omega}{\Omega_i} k \frac{H(\omega)}{\rho} \left[e^{ikr} - e^{ik(z+a-d)} \right] \quad \rho < a \quad (28b)$$

and

$$\tilde{B}_\varphi = - \frac{\omega}{\Omega_i} \frac{k}{S} \frac{H(\omega)}{\rho} \cos \theta e^{ikr} \quad \rho > a \quad (29a)$$

$$= - \frac{\omega}{\Omega_i} \frac{k}{S} \frac{H(\omega)}{\rho} \left[\cos \theta e^{ikr} - e^{ik(z+a-d)} \right] \quad \rho < a \quad (29b)$$

Hence, for $\rho > a$, the relative phases of the waves traveling in the plus and minus z directions vary with ρ in such a manner that the net effect is to produce a spherical wave. The wave amplitudes decrease with distance from the z axis, but not with z , and for sufficiently large z , $|\tilde{E}_\rho|$ can be comparable to $|\tilde{E}_\varphi|$. The total electric field for $\rho > a$ is then

$$\tilde{E} = \frac{H(\omega) e^{ikr}}{r} \left\{ \left[\frac{1}{r} - ik \right] \sin \theta \frac{e}{\varphi} - \frac{\omega k}{\Omega_i \sin \theta} \frac{e}{\rho} \right\} \quad (30)$$

For $kr \gg 1$ the polarization is

$$P = \frac{iE_\rho}{E_\varphi} = \frac{\omega/\Omega_i}{\sin^2 \theta} \quad (31)$$

For $\sin^2 \theta \ll \omega/\Omega_i$ and $\rho > a$, the electric field is essentially given by Eq. (28a). For approximately the same range of θ the plane wave normal modes are circularly polarized.* The amplitude of these modes

*See Ref. 12, p. 43.

can be related to the source fields by writing Eq. (28a) as the sum of a left and right circularly polarized wave, each of magnitude $\frac{1}{2} |E_\rho|$.

Finally, the magnitude of the electric fields inside the cylinder $\rho = a$ (i.e., $\sin \theta < a/r$) will be reduced from those outside by the factor

$$k[r-z-(a-d)] \leq k\left[\frac{a^2}{2r} - (a-d)\right]$$

(valid for $r \gg a$, $k(a-d) \ll 1$). The two waves in the region $\rho < a$ thus interfere destructively for the long wavelengths of interest here.

VII. CONCLUSIONS

In this Memorandum, a theory is proposed for the generation of the waves responsible for the prompt magneto-telluric effects of high-altitude nuclear explosions. A theoretical dependence of the amplitude of the generated signal on the yield-to-mass ratio of the device is obtained (for expansion speeds less than the Alfven velocity) as well as the power spectral density and the fraction of hydromagnetic energy which appears as MHD radiation. In particular, for a given hydromagnetic yield Y_H and Alfven speed S , the theory predicts that the smaller the mass of the device, the stronger the MHD signal produced, and therefore the easier it will be to detect. The theory also predicts a dipole radiation pattern having maximum intensity perpendicular to the external magnetic field, with most of the energy appearing in the isotropic mode. The experimental data from Argus, however, show that the maximum ground signal appears in the direction of the field lines passing through the burst. In order to compare the signals computed here with experiment, it is necessary also to consider the filtering effects of the earth-ionosphere-exosphere system. It has been pointed out, for example, that inhomogeneities in the propagation medium could couple the isotropic to the anisotropic mode which propagates along the field lines. At least for plane waves, the transmission coefficient for the anisotropic mode has been shown to dominate that of the isotropic mode.^(4,5) If a similar domination holds for the spherical modes generated by this model, it might explain the apparent discrepancy. It is thus proposed that, as far as is profitable, the effects of propagation of these waves through the earth-ionosphere-exosphere system be incorporated into this analysis.

Appendix A

CALCULATION OF THE ZERO-ORDER FIELDS

Because the problem is an initial value problem with E_φ and its time derivatives all initially equal to zero, Eq. (4a) can be regarded as a Laplace transformed equation for E_φ with transformation variable $i\omega$. The unperturbed vector potential at infinity is $\underline{A}^0 = \frac{1}{2} B_0 r \sin \theta \underline{e}_\varphi$. The solution of Eq. (5a) representing outgoing waves and varying as $\sin \theta$ (from continuity of \underline{A} at $r = St$) is⁽¹⁹⁾

$$\tilde{E}_\varphi(r, \theta, i\omega) = K \tilde{F}(i\omega) \left[\frac{1}{r^2} - \frac{i\omega}{Sr} \right] e^{i\omega r/S} \sin \theta \quad (A-1)$$

where \tilde{F} is an arbitrary function of its argument and K is a constant.

Inverting Eq. (A-1) yields

$$E_\varphi(r, \theta, t) = K \left[\frac{F(t-r/S)}{r^2} + \frac{F'(t-r/S)}{Sr} \right] \sin \theta$$

where $F(t)$ is in the inverse transform of the function \tilde{F} , and the prime denotes a time derivative. Choosing a Coulomb gauge, and defining $\eta = t-r/S$, the corresponding vector potential is

$$\underline{A} = A_\varphi \underline{e}_\varphi = \frac{1}{2} B_0 \sin \theta \left[r - \left(\frac{f(\eta)}{r^2} + \frac{f'(\eta)}{Sr} \right) \right] \underline{e}_\varphi \quad (A-2)$$

where $f(\eta) = \partial F / \partial \eta$, and the constant K has been chosen such that

$A_\varphi(r, \theta, t) \rightarrow \frac{1}{2} B_0 r \sin \theta$ as $r \rightarrow \infty$. The condition $B_r = 0$ (Eq. (6a)) at the surface of the sphere implies, with Eq. (A-2), that A_φ vanish there, and the continuity of \underline{A} at $r = St$ implies $f(0) = f'(0) = 0$.

First, consider the period from $t = 0$ to $t = \tau$ when the sphere is expanding. At the surface, $r = Vt$, and $\eta = \frac{r}{S} \left(\frac{1-\beta}{\beta} \right)$, where $\beta = V/S$. Hence, from Eq. (A-2), f must satisfy the differential equation

$$f'(\eta) + \frac{S}{r} f(\eta) - Sr^2 = 0$$

at

$$r = \frac{\beta S \eta}{1-\beta}$$

or

$$f'(\eta) + \left(\frac{1-\beta}{\beta} \right) \frac{1}{\eta} f(\eta) = \frac{\beta^2 S^3 \eta^2}{(1-\beta)^2} \quad (\text{A-3})$$

The required solution is

$$f(\eta) = \frac{S^3 \beta^3 \eta^3}{(1-\beta)^2 (1+2\beta)} \quad (\text{A-4})$$

and hence the vector potential valid for $0 < \eta < (1-\beta)\tau$, denoted by

A_{φ}^{I} , is

$$A_{\varphi}^{\text{I}} = \frac{1}{2} B_0 \sin \theta \left[r - \frac{\beta^3 S^3}{(1-\beta)^2 (1+2\beta)} \left(\frac{\eta^3}{r^2} + \frac{3\eta^2}{rS} \right) \right] \quad (\text{A-5})$$

The vector potential after the sphere has stopped (time τ , radius $a = \beta S\tau$) may be written, as in Eq. (A-2),

$$A_{\varphi}^{\text{II}} = \frac{1}{2} B_0 \sin \theta \left[r - \left(\frac{g(\eta)}{r^2} + \frac{g'(\eta)}{rS} \right) \right] \quad (\text{A-6})$$

Again, applying the condition $A_\varphi = 0$ at $r = a$ implies $g(\eta)$ satisfy

$$g'(\eta) + \frac{S}{a} g(\eta) = a^2 S \quad (\text{A-7})$$

which has the solution

$$g(\eta) = a^3 + C e^{-\eta/\beta\tau} \quad (\text{A-8})$$

The time it takes the signal that the sphere has stopped to reach a distance r is $t = \tau + (r-a)/S$, or $\eta = (1-\beta)\tau$. Equating A^I and A^{II} at $\eta = (1-\beta)\tau$ shows that the following two equations must be satisfied

$$a^3 + C e^{-\left(\frac{1-\beta}{\beta}\right)} = \frac{a^3(1-\beta)}{1+2\beta} \quad (\text{A-9a})$$

$$-\frac{1}{\beta\tau} C e^{-\left(\frac{1-\beta}{\beta}\right)} = \frac{3\beta^3 S^3 \tau^2}{(1-\beta)^2 (1+2\beta)} \quad (\text{A-9b})$$

Both equations yield $C = \frac{-3\beta a^3}{1+2\beta} e^{\left(\frac{1-\beta}{\beta}\right)}$, and therefore

$$g(\eta) = a^3 \left\{ 1 - \frac{3\beta}{1+2\beta} e^{-\left[\frac{\eta-(1-\beta)\tau}{\beta\tau}\right]} \right\} \quad (\text{A-10})$$

Hence,

$$A^{II} = \frac{1}{2} B_o r \sin \theta \left(1 - \frac{a^3}{r^3} \right) + \frac{3}{2} \frac{B_o \beta a \sin \theta}{1+2\beta} \left(\frac{a^2}{r^2} - \frac{a}{r} \right) e^{-\left[\frac{\eta-(1-\beta)\tau}{\beta\tau}\right]} \quad (\text{A-11})$$

The zero-order fields in Eqs. (7) and (8) are then found from the relations

$$E_{\varphi} = - \frac{\partial A}{\partial \eta} \quad (\text{A-12a})$$

$$B_r = \frac{2}{r} A \cot \theta \quad (\text{A-12b})$$

$$B_{\theta} = - \frac{1}{r} \frac{\partial}{\partial r} (rA) \quad (\text{A-12c})$$

All other components of the field quantities are zero.

Appendix B

DIRECT CALCULATION OF THE WORK DONE IN EXPANDING
THE SPHERE FROM THE STRESS TENSOR

Consider a mathematical sphere of radius R , where $V_t < R < V_T = a$, concentric with the conductor. For a linear dielectric medium, the volume forces may be expressed in terms of the fields by*

$$\underline{F} = \int \underline{f} \, dV = \int \underline{T} \cdot d\underline{S} - \frac{\partial}{\partial t} \int (\epsilon \underline{E} \times \underline{B}) dV \quad (B-1)$$

where \underline{T} is the Maxwell stress tensor and is integrated over the surface bounding the volume V . Applied to the mathematical sphere, Eq. (C-1) states that the volume force acting on the currents within the sphere is equal to the total stress transferred across the surface minus the rate at which electromagnetic momentum ($\epsilon \underline{E} \times \underline{B}$) is being lost from the enclosed volume. The force acting on the conductor for any $r(< a)$ is then given by Eq. (C-1) evaluated at $r = R$ and $t = R/V$.

To compute the first term, consider a local Cartesian coordinate system fixed on sphere R with axes (x, y, z) along the directions $(\underline{e}_r, \underline{e}_\theta, \underline{e}_\phi)$, respectively. Then $E \rightarrow E_z$, $B \rightarrow B_y$, and the stress transmitted across the surface element $d\underline{S}$ is $-\left[\epsilon E^2/2 + B^2/2\mu_0\right] d\underline{S} \underline{e}_x$. Substituting the fields from Eqs. (7) and (8) and integrating over the surface yields

$$\int \underline{T} \cdot d\underline{S} = - \frac{3\pi B_o^2}{\mu_0} \frac{(1+\beta)^2 (1+\beta^2)}{(1-\beta)^2 (1+2\beta)^2} R^2 \underline{e}_r \quad (B-2)$$

for the stress at $r = R$.

* See Ref. 14, p. 112 ff.

From Eqs. (7) and (8) the electromagnetic momentum density is given by

$$\epsilon \underline{E} \times \underline{B} = \frac{3}{4S} \frac{B_o^2}{\mu_o} \frac{\beta^3}{(1-\beta)^2(1+2\beta)} \sin^2 \theta \left\{ \left[w^3 + 2w \right] \left[2 + \frac{\beta^3}{(1-\beta)^2(1+2\beta)} \right. \right. \\ \left. \left. (w^3 + 3w^2 + 6w) \right] \right\} \quad (B-3)$$

where $w = \eta S/r$. The integration over the volume between the conductor and the sphere R leads to

$$\int (\epsilon \underline{E} \times \underline{B}) dV = K \underline{e}_r \int_{Vt}^R dr \left\{ r^2 w \left[\frac{\beta^3}{(1-\beta)^2(1+2\beta)} (w^4 + 5w^3 + 12w + 12) \right. \right. \\ \left. \left. + (2w + 4) \right] \right\} \quad (B-4)$$

where

$$K = \frac{2\pi B_o^2}{\mu_o S} \frac{\beta^3}{(1-\beta)^2(1+2\beta)}$$

Differentiating under the integral sign:

$$\left[\frac{\partial}{\partial t} \int (\epsilon \underline{E} \times \underline{B}) dV \right]_{\substack{t=R/V \\ r=R}} = -KV \left\{ \right\}_{\substack{r=R \\ w=\left(\frac{1-\beta}{\beta}\right)}} \underline{e}_r \quad (B-5)$$

where $\left\{ \right\}$ denotes the integrand in Eq. (B-4). Carrying out the algebra yields

$$\left[\frac{\partial}{\partial t} \int (\epsilon \underline{E} \times \underline{B}) dV \right]_{\substack{t=R/V \\ r=R}} = - \frac{6\pi B_o^2 \beta^2 (1+\beta)^2 R^2}{\mu_o (1-\beta)^2 (1+2\beta)^2} \underline{e}_r \quad (B-6)$$

Substituting Eqs. (B-2) and (B-6) into Eq. (B-1) yields

$$\underline{F} = - \frac{3\pi B_o^2}{\mu_o} \frac{(1+\beta)^3}{(1-\beta)(1+2\beta)^2} R^2 \underline{e}_r \quad (B-7)$$

Integrating over R from 0 to a gives Eq. (21) for the total work done in expanding the sphere.

Appendix C

CALCULATION OF THE FIRST-ORDER FIELDS

In cylindrical coordinates, Eq. (5b) is

$$\frac{\partial^2 \mu}{\partial z^2} + k^2 \mu = F(\omega) e^{ik(\rho^2 + z^2)^{\frac{1}{2}}} \frac{\rho}{\rho^2 + z^2} \left[\frac{1}{(\rho^2 + z^2)^{\frac{1}{2}}} - ik \right] \equiv P(\omega, \rho, z) \quad (C-1)$$

where $\tilde{E}_\rho = \mu$, and $F(\omega) = (i\omega^3 / \Omega_1 S^2) H(\omega)$. The Green's function is the solution of

$$\frac{\partial^2 G}{\partial z^2} + k^2 G = \delta(z - z') \delta(\rho - \rho') \quad (C-2)$$

subject to the appropriate boundary conditions.

SOLUTION FOR $\rho > a$

The solution of Eq. (C-2) for an infinite "string" yielding only outgoing waves at infinity is

$$G_1 = \frac{1}{2ik} e^{-ik(z-z')} \delta(\rho - \rho') \quad z < z' \quad (C-3a)$$

$$G_2 = \frac{1}{2ik} e^{ik(z-z')} \delta(\rho - \rho') \quad z > z' \quad (C-3b)$$

The solution of Eq. (C-1) for $\rho > a$ is then

$$\begin{aligned} \mu &= \int_{a-\infty}^{\infty} \int_{-\infty}^z G_2(\rho - \rho', z - z') P(\omega, \rho', z') dz' d\rho' + \int_{a-\infty}^{\infty} \int_z^{\infty} G_1(\rho - \rho', z - z') P(\omega, \rho', z') dz' d\rho' \\ &= \int_{-\infty}^z \frac{e^{ik(z-z')}}{2ik} P(\omega, \rho, z') dz' + \int_z^{\infty} \frac{e^{-ik(z-z')}}{2ik} P(\omega, \rho, z') dz' \end{aligned} \quad (C-4)$$

Substituting for P from Eq. (C-1) and letting $x = z'/\rho$ yields

$$\mu = \frac{F(\omega)}{2} \left\{ e^{ikz} \int_{-\infty}^{z/\rho} \frac{e^{ik\rho[(1+x^2)^{\frac{1}{2}}-x]}}{1+x^2} \left[\frac{1}{ik\rho(1+x^2)^{\frac{1}{2}}} - 1 \right] dx \right. \\ \left. + e^{-ikz} \int_{z/\rho}^{\infty} \frac{e^{ik\rho[(1+x^2)^{\frac{1}{2}}+x]}}{1+x^2} \left[\frac{1}{ik\rho(1+x^2)^{\frac{1}{2}}} - 1 \right] dx \right\} \quad (C-5)$$

Letting $x \rightarrow -x$ in the second integral shows that the second expression is equal to the first with $z \rightarrow -z$. Substituting $y = (1+x^2)^{\frac{1}{2}}-x$ the first expression can be written as

$$2e^{ikz} \int_{\gamma}^{\infty} \frac{e^{ik\rho y}}{1+y^2} \left[\frac{2y}{ik\rho(1+y^2)} - 1 \right] dy$$

where $\gamma = (1+z^2/\rho^2)^{\frac{1}{2}} - z/\rho = \frac{r-z}{\rho}$. Integrating $\int_{\gamma}^{\infty} \frac{e^{ik\rho y}}{(1+y^2)} dy$ by parts reveals that the above integral is equal to $\frac{e^{ik\rho\gamma}}{ik\rho(1+\gamma^2)}$.

Therefore,

$$\mu = \frac{F(\omega)}{ik\rho} e^{ikr} \left\{ \frac{1}{1+\left(\frac{r-z}{\rho}\right)^2} + \frac{1}{1+\left(\frac{r+z}{\rho}\right)^2} \right\} = \frac{F(\omega)e^{ikr}}{ik\rho} \quad (C-6)$$

SOLUTION FOR $\rho < a$

The retarded solution of Eq. (C-2) for $z > 0$ with $G = 0$ at $z = d = (a^2 - \rho^2)^{\frac{1}{2}}$ is

$$G_1(\rho - \rho', z - z') = \frac{1}{2ik} \left[e^{-ik(z-z')} - e^{ik(z+z'-2d)} \right] \delta(\rho - \rho') \quad d < z < z' \quad (C-7a)$$

$$G_2(\rho-\rho', z-z') = \frac{1}{2ik} \left[e^{ik(z-z')} - e^{ik(z+z'-2d)} \right] \delta(\rho-\rho') \quad z > z' \quad (C-7b)$$

The solution of Eq. (C-1) for $\rho < a$ is then

$$\begin{aligned} \frac{e^{ikz}}{2ik} & \left[\int_d^z e^{-ikz'} P dz' - e^{-2ikd} \int_d^z e^{ikz'} P dz' - e^{-2ikd} \int_z^\infty e^{ikz'} P dz' \right] \\ & + \frac{e^{ikz}}{2ik} \int_z^\infty e^{ikz'} P dz' \end{aligned} \quad (C-8)$$

Substituting for P from Eq. (C-1) yields

$$\begin{aligned} \mu = \frac{F(\omega)}{2} & \left\{ e^{ikz} \int_{d/\rho}^{z/\rho} \frac{e^{ik\rho[(1+x^2)^{\frac{1}{2}}-x]}}{1+x^2} \left[\frac{1}{ik\rho(1+x^2)^{\frac{1}{2}}} - 1 \right] dx \right. \\ & \left. + \left(-e^{ik(z-2d)} \int_{d/\rho}^\infty + e^{-ikz} \int_{z/\rho}^\infty \right) \frac{e^{ik\rho[(1+x^2)^{\frac{1}{2}}+x]}}{1+x^2} \left[\frac{1}{ik\rho(1+x^2)^{\frac{1}{2}}} - 1 \right] dx \right\} \end{aligned} \quad (C-9)$$

The integrals are essentially the same as in Eq. (C-5) and yield

$$\begin{aligned} \mu = \frac{F(\omega)}{ik\rho} & \left\{ e^{ikz} \left[\frac{e^{ik(r-z)}}{1 + \left(\frac{r-z}{\rho}\right)^2} - \frac{e^{ik(a-d)}}{1 + \left(\frac{a-d}{\rho}\right)^2} \right] - e^{ik(z-2d)} \left[\frac{e^{ik(a+d)}}{1 + \left(\frac{a+d}{\rho}\right)^2} \right] \right. \\ & \left. + e^{-ikz} \left[\frac{e^{ik(r+z)}}{1 + \left(\frac{r+z}{\rho}\right)^2} \right] \right\} = \frac{F(\omega)}{ik\rho} \{ e^{ikr} - e^{ik(z+a-d)} \} \end{aligned} \quad (C-10)$$

The solution for $z < 0$ is identical to Eq. (C-10) with $z \rightarrow -z$.

REFERENCES

1. Francis, W. E., and R. Karplus, "Hydromagnetic Waves in the Ionosphere," J. Geophys. Res., Vol. 65, No. 11, 1960, p. 3593.
2. Jacobs, J. A., and T. Watanabe, "Propagation of Hydromagnetic Waves in the Lower Exosphere and the Origin of Short Period Geomagnetic Micropulsations," J. Atmos. Terrest. Phys., Vol. 24, 1962, pp. 413-434.
3. Prince, C. E., Jr., and F. X. Bostick, Jr., "Ionospheric Transmission of Transversely Propagated Plane Waves at Micropulsation Frequencies and Theoretical Power Spectrums," J. Geophys. Res., Vol. 69, August 1, 1964, p. 3213.
4. Field, E. C., and C. Greifinger, "Transmission of Geomagnetic Micropulsations through the Ionosphere and Lower Exosphere," J. Geophys. Res., Vol. 70, No. 19, 1965, p. 4885; also published by The RAND Corporation, RM-4494-PR, March 1965.
5. Field E. C., and C. Greifinger, "Equatorial Transmission of Geomagnetic Micropulsations through the Ionosphere and Lower Exosphere," J. Geophys. Res., Vol. 71, No. 13, 1966, p. 3223; also published by The RAND Corporation, RM-4858, February 1966.
6. Prince, C. E., F. X. Bostick, and H. W. Smith, "Impulse Response of the Magnetospheric Column," J. Geophys. Res., Vol. 70, October 1, 1965, p. 4901.
7. Field, E. C., and C. Greifinger, "Ground Level Magnetic Fluctuations Due to High Altitude Nuclear Bursts or Impulse Sources of Natural Origin," J. Geophys. Res., Vol. 72, No. 1, 1967; also published by The RAND Corporation, RM-4946-ARPA, March 1966.
8. Berthold, W. K., A. K. Harris, and H. J. Hope, "World-Wide Effects of Hydromagnetic Waves Due to Argus," J. Geophys. Res., Vol. 65, August 1960, p. 2233.
9. Caner, B., Prompt World-Wide Geomagnetic Effects of High-Altitude Nuclear Explosions, Publications of the Dominion Observatory, Ottawa, Vol. XXXI, No. 1, 1964.
10. Leipunskii, O. I., "Possible Magnetic Effects from High-Altitude Explosions of Atomic Bombs," J. Exptl. Theoret. Phys. (USSR), Vol. 38, January 1960, p. 219.
11. Bernstein, I. B., and R. M. Kulsrud, The Uniform Expansion of a Spherical Plasma Bubble into an Ionized Atmosphere in a Strong Magnetic Field, Air Force Special Weapons Center, Report AFSWC-TDR-62-12, Vol. II, 1962, Chapter 3.
12. Stix, T. H., The Theory of Plasma Waves, McGraw-Hill Book Company, Inc., New York, 1962, p. 10.

13. Karplus, R., "Radiation of Hydromagnetic Waves," Phys. Fluids, Vol. 3, No. 5, 1960, p. 800.
14. Panofsky, W., and M. Phillips, Classical Electricity and Magnetism, Addison-Wesley Publishing Company, Inc., Reading, Massachusetts, 1955, p. 144.
15. Landau, L. D., and E. M. Lifschitz, Electrodynamics of Continuous Media, Addison-Wesley Publishing Company, Inc., Reading, Massachusetts, 1960, p. 129.
16. Gilinsky, V., and D. Holliday, Interaction Energy of a Dielectric in an Electrostatic Field, The RAND Corporation, RM-4892-PR, March 1966.
17. Glasstone, S. (ed.), The Effects of Nuclear Weapons, United States Atomic Energy Commission, Washington, D. C., 1962, p. 50.
18. Lapp, R. E., "Nuclear Weapons Systems," Bull. Atomic Scientists, Vol. XVII, February 1961, p. 99.
19. Venezian, G., Radiation Due to the Motion of a Conducting Sphere in a Magnetic Field, California Institute of Technology, Division of Engineering and Applied Sciences, Report 85-25, 1963, p. 39.